International Atomic Energy Agency

INDC(GDR)-058/L

INDC INTERNATIONAL NUCLEAR DATA COMMITTEE

THE NEUTRON EMISSION CROSS SECTION OF VANADIUM, TANTALUM AND TUNGSTEN AT 14 MeV NEUTRON INCIDENCE ENERGY

H. Al Obiesi, T. Elfruth, T. Hehl, M. Toepfer, D. Seeliger,
K. Seidel, S. Unholzer
Technische Universität Dresden, GDR

September 1990

IAEA NUCLEAR DATA SECTION, WAGRAMERSTRASSE 5, A-1400 VIENNA

INDC(GDR)-058/L

THE NEUTRON EMISSION CROSS SECTION OF VANADIUM, TANTALUM AND TUNGSTEN AT 14 MeV NEUTRON INCIDENCE ENERGY

H. Al Obiesi, T. Elfruth, T. Hehl, M. Toepfer, D. Seeliger,
K. Seidel, S. Unholzer
Technische Universität Dresden, GDR

September 1990

Reproduced by the IAEA in Austria
September 1990

90-04592

THE NEUTRON EMISSION CROSS SECTION OF VANADIUM, TANTALUM AND TUNGSTEN AT 14 MeV NEUTRON INCIDENCE ENERGY *)

H. Al Obiesi, T. Elfruth, T. Hehl, M. Toepfer, D. Seeliger,
K. Seidel, S. Unholzer
Technische Universität Dresden, Sektion Physik
Mommsenstr. 13, Dresden, DDR-8027,

Abstract

Double-differential neutron cross section of Vanadium, Tantalum and Tungsten at 14 MeV incidence energy have been measured using the TUD time-of flight spectrometer. The experimentally obtained data are compared with previous results of experiments as well as with ENDF/B-IV data and with caculations using the SMD/SMC-model code EXIFON.

1. Introduction

Vanadium (V) , Tantalum (Ta) and Tungsten (W) are used in fusion reactor designs as structural and shielding materials. Due to the location of this materials also near by the DT-neutron source the double-differential neutron emission cross section (DDX) of V, Ta and W at 14 MeV incidence energy are of special importance. In the WRENDA-List 1987/88 (World Request List for Nuclear Data) /1/ accuracies of 10% for W (priority 1) and 15% for V and Ta (priority 1 and 2, respectively) are demanded. Besides a good knowledge of the spectral shape of the energy differential neutron emission taking into account direct and other preequilibrium contributions the angular distributions of the neutron emission have to be well determined.

In almost all of the evaluated data library files for V, Ta and W (see e.g. ENDF/B-IV) preequilibrium contributions in the high energy part of the neutron emission spectra are neglected or are underestimated. Angular distributions of inelastic scattered neutrons are assumed to be isotropic with exception of the scattering from only a few low-lying levels. In the frame of the IAEA Co-ordinated Research Program (CRP) on measurement and

*) This work was done in the frame of the IAEA Co-ordinated Research Program on "Measurement and analysis of 14 MeV neutron-induced double-differential neutron emission cross sections needed for fission und fusion reactor technology.

analysis of 14 MeV neutron-induced double- differential neutron emission cross sections needed for fission and fusion reactor technology DDX for V, Ta and W were measured at the 14 MeV neutron generator of the Dresden University using the installed time-of-flight spectrometer which was particularly constructed to study the angular distribution of the neutron emission at 14 MeV incidence energy.

2. Experiment and data processing

The geometrical arrangement of the DDX experiment is shown in Fig. 1. The choosen ring geometry with flight path perpendicular to the deuteron beam direction, the construction of collimator channel, shadow bar and sample ring and the diameter of the neutron source allows the measurement at neutron emission angles ϑ between 15° and 165°. The distance between target and detector is 4.8 m.

The neutron generator working in the pulsed regime with deuteron pulses of 2 ns f.w.h.m. and repetition rates of 2.5 or 5 MHz, respectively, produces $2...5 * 10^{9}$ neutrons/s on a TiT-target for a mean deuteron beam currentof 30 μA. The source strength is determined by counting the α-particles of the source reaction with a silicon surface-barrier detector at an angle of $\phi_{o} = 166^{o}$ with respect to the deuteron beam direction.

A scintillation detector and a long counter are used as relative monitors.

The anisotropy of the neutron source reaction is calculated with the QELL program /2/ taking into account the deacceleration of the deuterons in the thick Ti-T layer. This dependence as well as the influence of target tube, backing and cooling on the source neutron distribution are measured with activation foils and with a recoil proton counter biased at 10 MeV. The obtained source neutron distributions are averaged over those directions the neutrons of which strike on the ring sample. The result is a weak but symmetric dependence of the neutron incidence energy and of the source anisotropy correction on ϑ. A detailed description of the source strength determination is given in Ref./3/.

The ring samples with natural isotopic compositions have inner diameters of 8.0 cm and outer diameters of 12.0 cm. Their thicknesses in flight path direction are 1.04 cm for V, 0.65 cm for Ta and 0.61 cm for W, respectively, which correspond to about

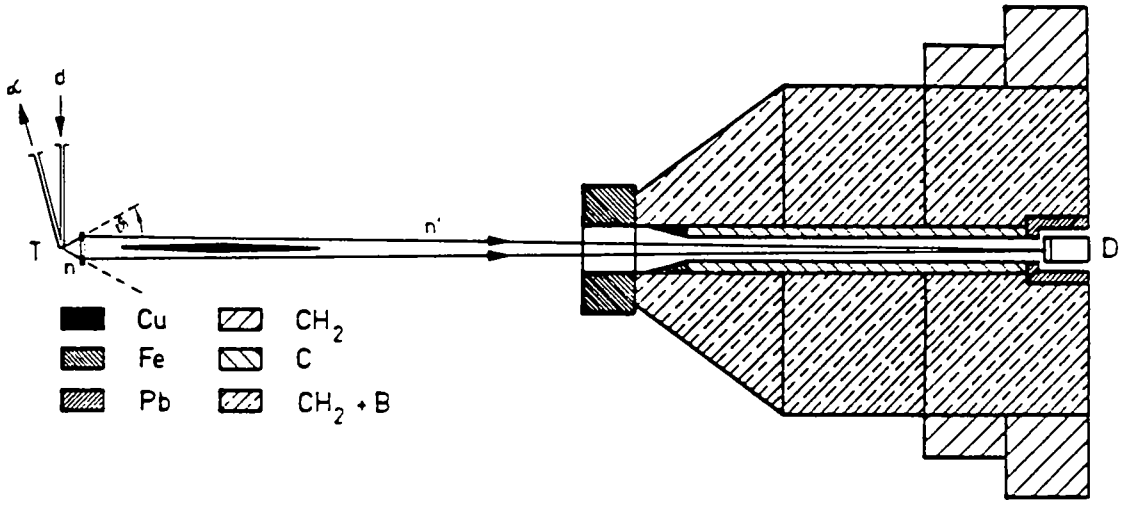

Fig.1

Geometrical arrangement of the time-of-flight spectrometer.
T, tritium target; D, neutron detector.

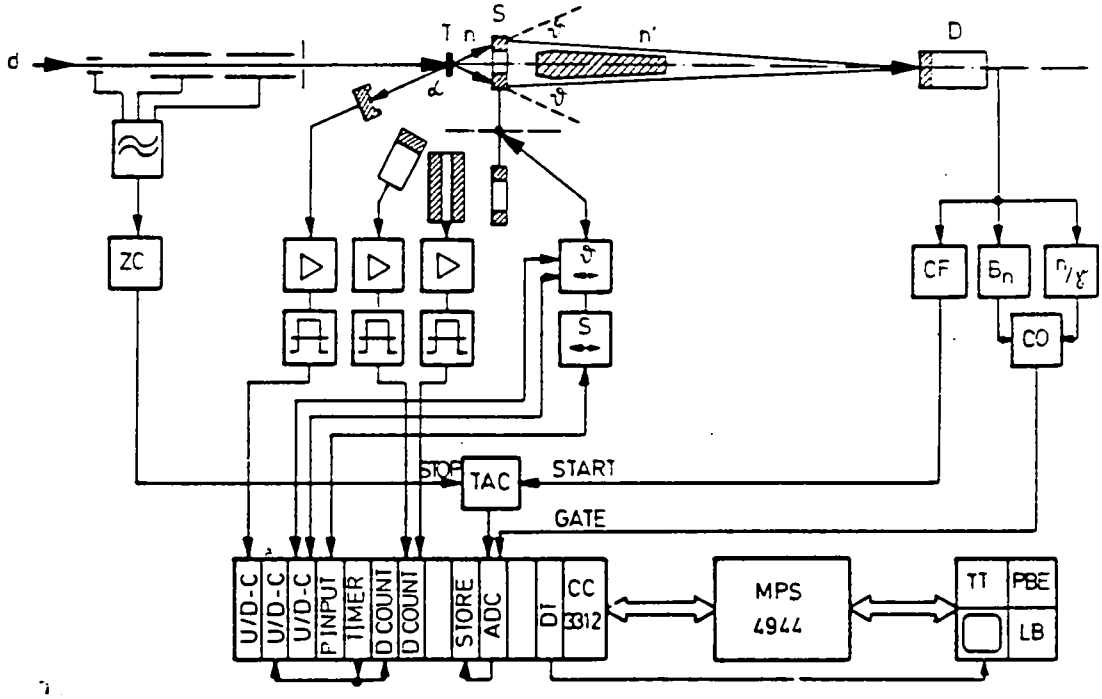

Fig. 2

Block scheme of the spectrometer
T, tritium target; S, sample; D, neutron detector;
ZC, zero-crossing trigger; CF, constant-fraction trigger;
B_n, proton-recoil-energy discriminator; CO, coincidence;
ϑ sample shifter; S, sample changer; TAC, time-to-amplitude converter; U/D-C, up-and-down counter; ADC, analog-to-digital converter; CC, controller of the CAMAC crate; MPS, microcomputer.

1/4 mean-free-path of the incoming source neutrons. At measurements around $\vartheta = 90^{o}$ a segment of 60° width is taken away from each sample.

The block scheme of the time-of-flight (TOF) spectrometer is shown in Fig. 2. The neutron TOF detector consists of a liquid NE-213 scintillator (4.5" diameter and 1.5" length) coupled to a XP 2041 photomultiplier. Its anode signals are used for timing, for neutron-gamma discrimination /4/ as well as for proton-recoil biasing. The neutron detector efficiency $\varepsilon(E)$ is measured by TOF-spectrometry of Cf-252 fission neutrons /5/, by a TOF neutron scattering experiment at hydrogen using a thin polyethylene ring as well as by the spectrometry of 14 MeV neutrons from the non-shadowed neutron source. Additionally $\varepsilon(E)$ is calculated with the Monte Carlo code NEUCEF /6/.

The TOF experiment is controlled by a microcomputer. Free programmable sample shifting (ϑ) and changing allows a subdivision in short-time data aquisition periods and a quasi-simultaneous measurement with and without sample over the whole angular range and a cycle-like repetition, many times. After inspection of the data of the short-time run and comparison with a reference spectrum obtained in the first cycle, the spectrum is summed up to the previous obtained correcting possible long-time shifts of the TOF spectrometer.

Measurements of TOF spectra are carried out for ϑ from 15° to 150°in steps of 15°.

The data processing consists of the following procedures:

- correction of the TOF-spectra for dead time and differential nonlinearity of the spectrometer;
- subtraction of the experimental background (without sample measurement and time uncorrelated background component);
- generation of the time scale starting from the centroid of the elastic scattering peak with the knowledge of the time channel width;
- time to energy transformation of the time spectra and scale;
- calculation of the neutron emission cross sections taking into account the geometrical relations (flight path, target-sample distance etc.), the sample mass and $\varepsilon(E)$;
- correction of the neutron source anisotropy;
- correction of the flux attenuation of incoming and outgoing neutron within the sample

- correction of multiple scattering calculated with the neutron transport code MORSE /7/ and with ENDF/B-IV data;
- transformation of DDX and energy scale in to center-of-mass system.

A detailed description of the data processing is given elsewhere (Ref. /3/).

3. Results

DDX in the center-of-mass system obtained for V, Ta and W from $\vartheta = 30^{o}$ up to 150° in steps of 15° in the emission energy interval from 1.4 MeV up to the incidence energy are given in the tables for 0.2 MeV averaging interval.
The uncertainties given in the tables include the statistical uncertainties only. The estimated systematic uncertainties are

source strength monitoring	: 4%
source anisotropy correction	: 2%
finite sample size correction	: 3%
(flux attenuation + multiple scattering)	
detector efficiency	: 5%
geometry dependend quantities	: 2%
(flight path, detector-front area,distance target-sample..)	

The angular resolution expressed as $\langle\Delta\vartheta^2\rangle^{1/2}$ are less than 4° in the whole angular range. The energy resolution is 3% at 3 MeV emission energy and 7% at 14 MeV.
In Figs. 3a)-g) examples of the present experimental DDX results are compared with results of the recent experiments of Takahashi /11-13/ and of Baba /14/ and with evaluated DDX from the ENDF/B-IV library. A deficit of inelastically scattered neutrons in the high-energy part of the ENDF/B-IV DDX of V and W is obvious, as well as the artificial spectral shape for Ta. Differences to the library data are apparent also in the low energy part of emission spectra.
An inprovement of the evaluated data can be achieved by adequate description of the reaction mechanisms contributing to the neutron emission spectrum.
As first step the DDX measured at 14 MeV are interpreted by calculations with the SMC/SMD model code EXIFON of Kalka/15/ in

which vibrational and single particle excitations are handled in a consistent way. The parameters used as code input are "global", that means the mean mass-number dependence of reaction cross section value, of single particle level density parameter, shell correction, deformation parameter etc. are used. Only one 2^+ and one 3^- vibrational excitation are taken into account. The low-lying rotational excitations in Ta and W are not handled. For the angular distribution of the neutron emission the Kalbach-Mann systematics /16/ is used.

To take into account the influence of the elastic scattering peak, due to the finite experimental resolution, on the high-energy part of the emission spectrum, the peak shape experimentally determined at $\vartheta = 15^{o}$ is used.

In Fig. 4,5,6 the results of the calculations are compared with the present experimental DDX and ENDF/B-IV data. The good overall description of the experimental DDX shows that the main reaction mechanisms are adequately taken into account. Further improvements are necessary especially for the description of the angular distributions in the high energy part of the emission spectrum, where the Kalbach-Mann systematics seems to be too crude.

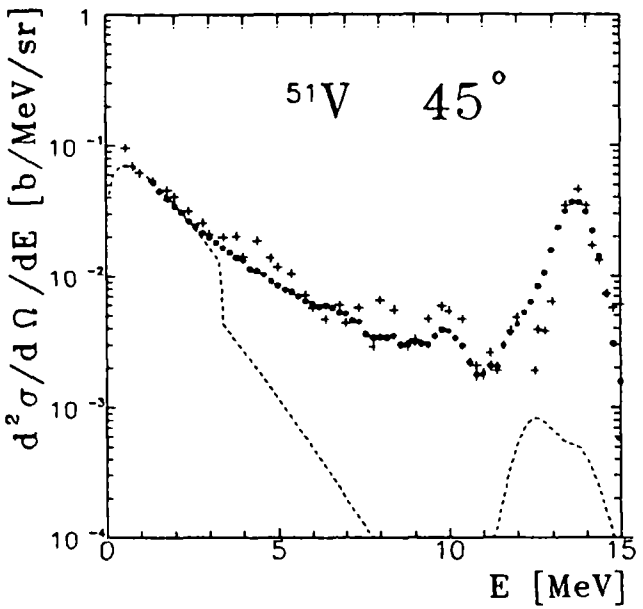

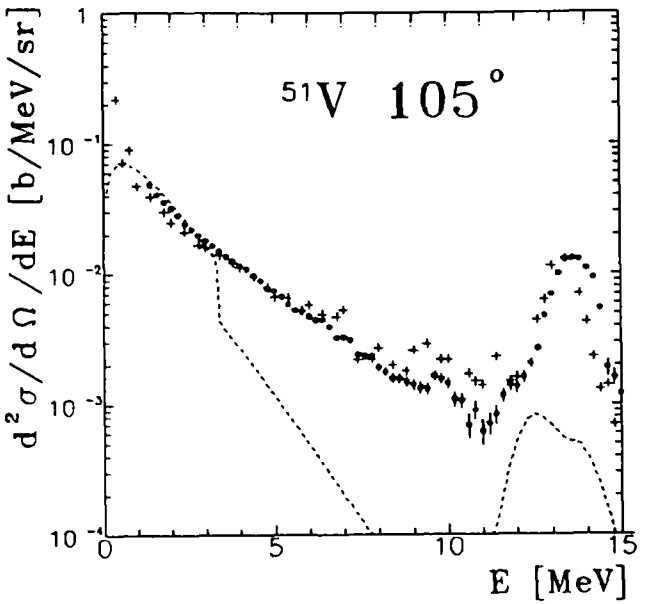

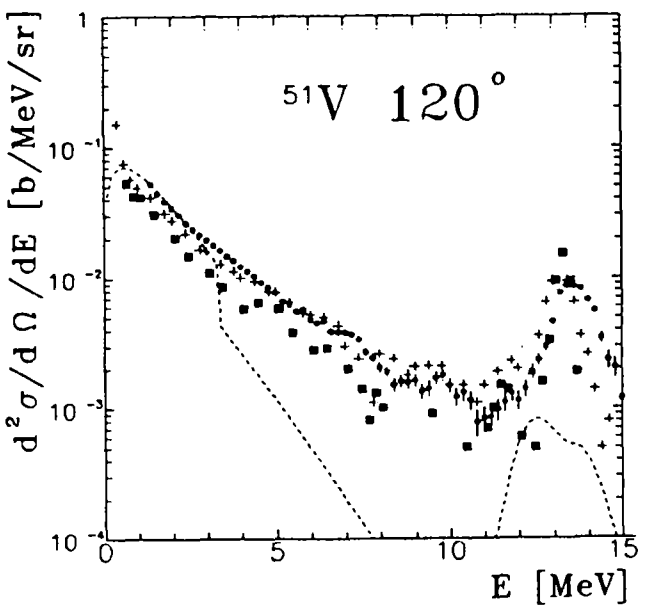

Fig. 3 a)-g)
Double-differential neutron emission cross sections of vanadium, tantalum and tungsten. Present experimental results (•) are compared with those of the recent experiments of Takahashi /11-13/ (■) and Baba /14/ (+), respectively, as well as data of the library ENDF/B-IV (dashed line).

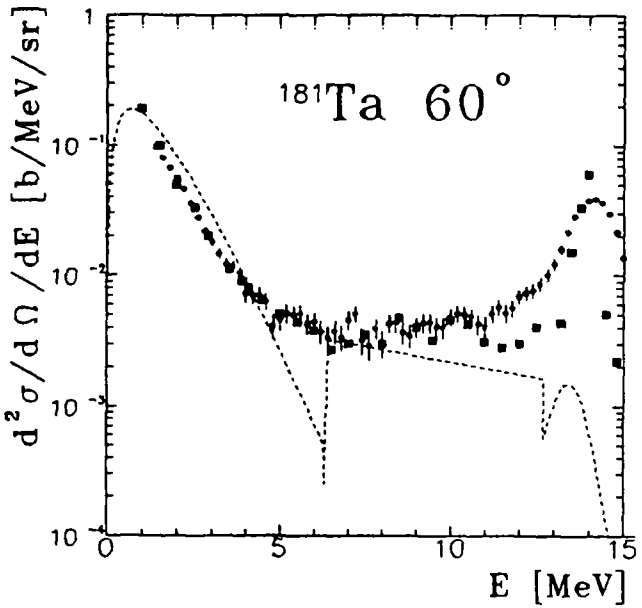
^{181}Ta 60°
$d^2\sigma/d\Omega/dE$ [b/MeV/sr]
E [MeV]

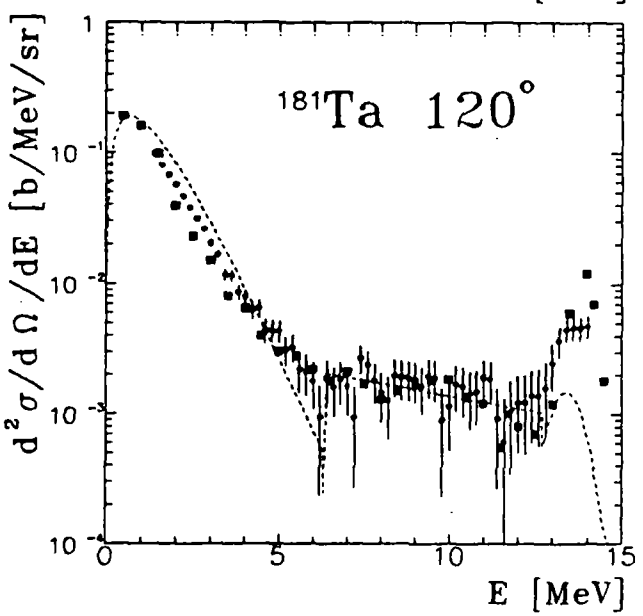
^{181}Ta 120°
$d^2\sigma/d\Omega/dE$ [b/MeV/sr]
E [MeV]

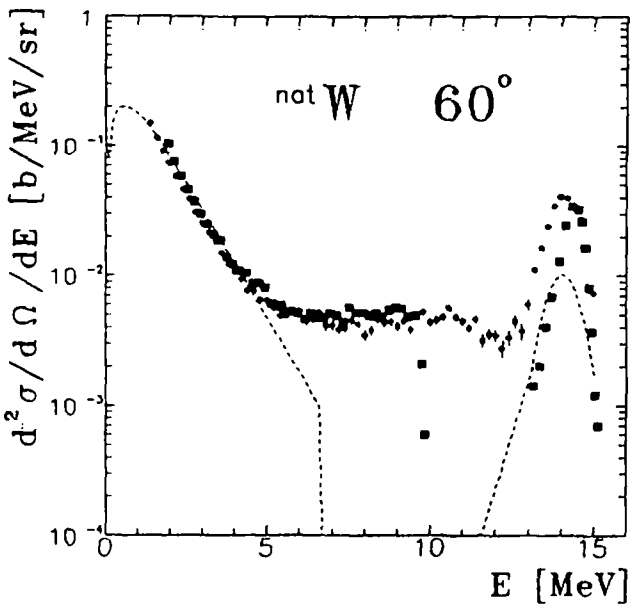
^{nat}W 60°
$d^2\sigma/d\Omega/dE$ [b/MeV/sr]
E [MeV]

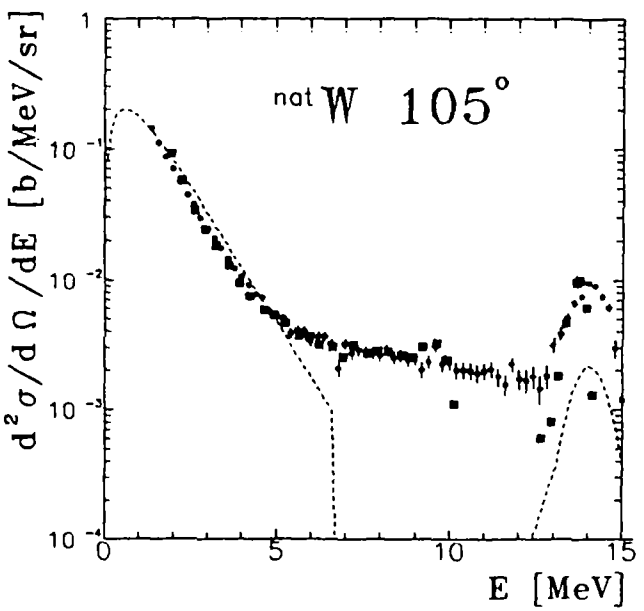
^{nat}W 105°
$d^2\sigma/d\Omega/dE$ [b/MeV/sr]
E [MeV]

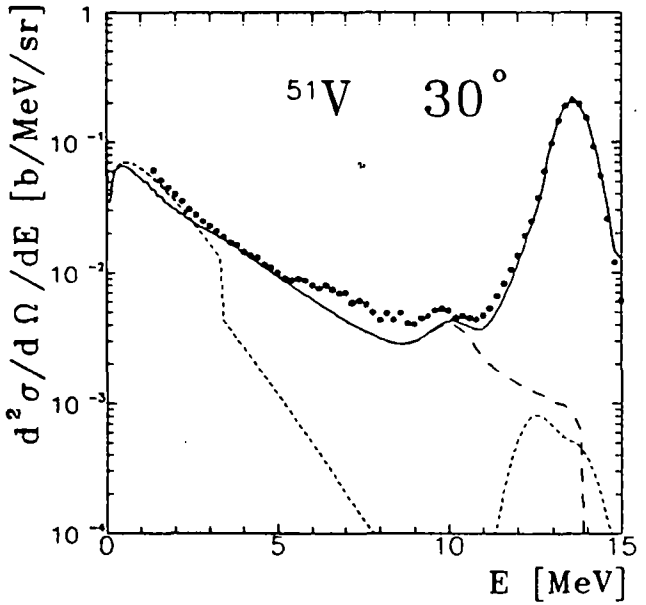

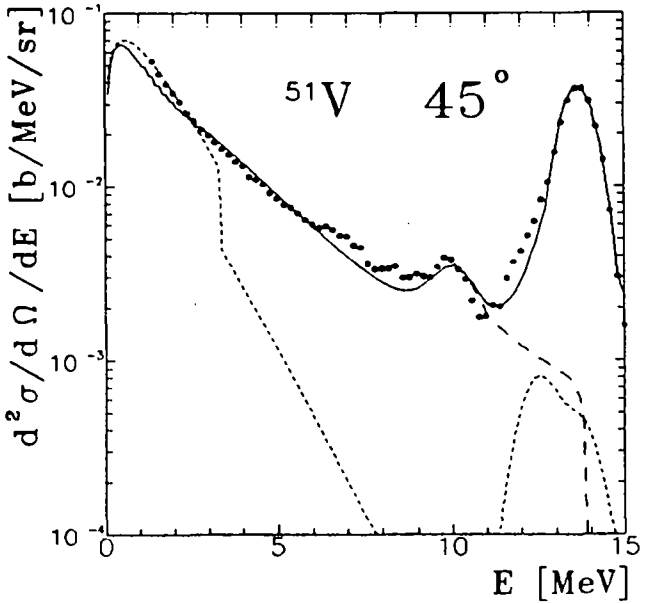

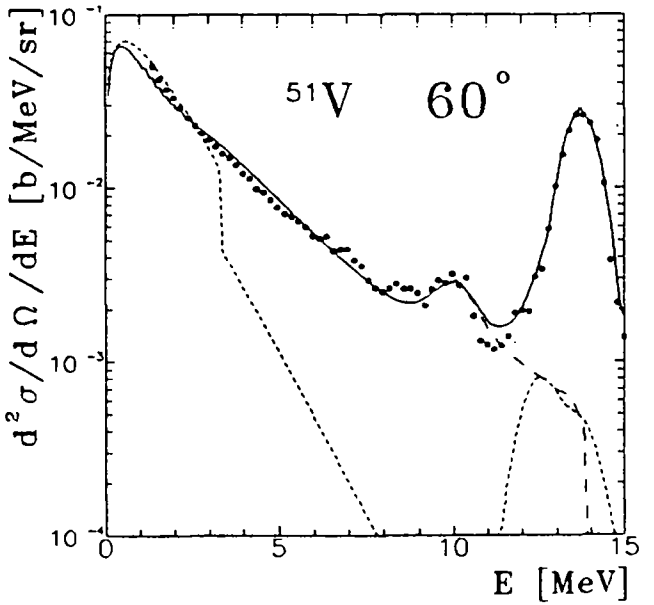

Fig. 4a)-i)

Double-differential neutron emission cross sections of vanadium at 14 MeV incidence energy.
Present experimental cross sections (•) are compared with ENDF/B-IV data (short-dashed line) and results of the EXIFON-calculation (long-dashed line). The solid line represents the sum of EXIFON results and the simulated elastic scattering peak.

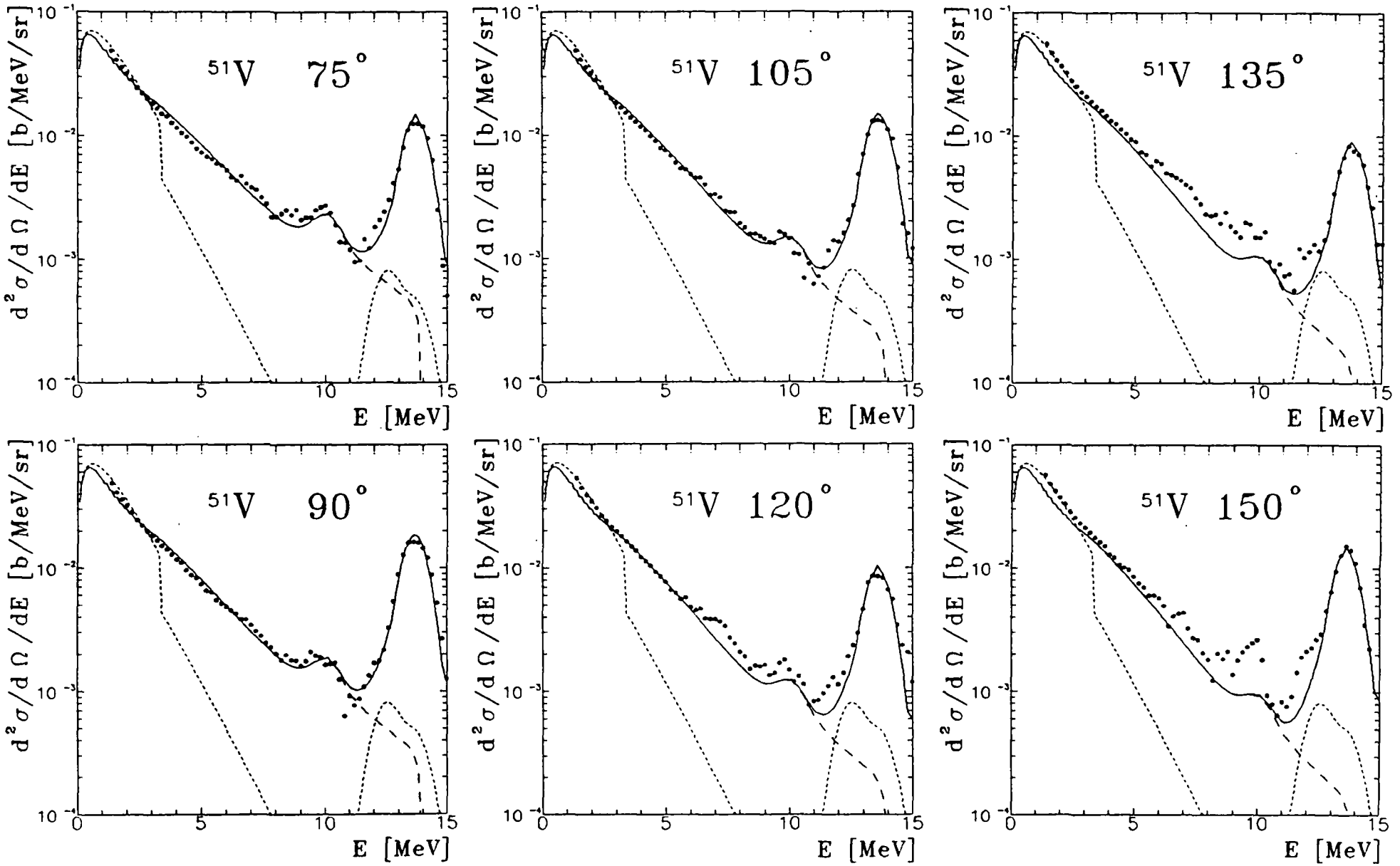
^{51}V 75°
^{51}V 105°
^{51}V 135°
^{51}V 90°
^{51}V 120°
^{51}V 150°
$d^2\sigma/d\Omega/dE$ [b/MeV/sr]
E [MeV]
10^{-1}
10^{-2}
10^{-3}
10^{-4}
0
5
10
15

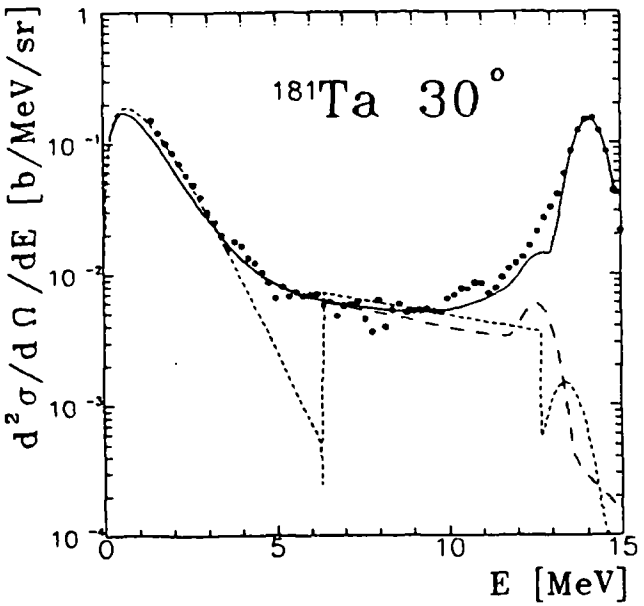

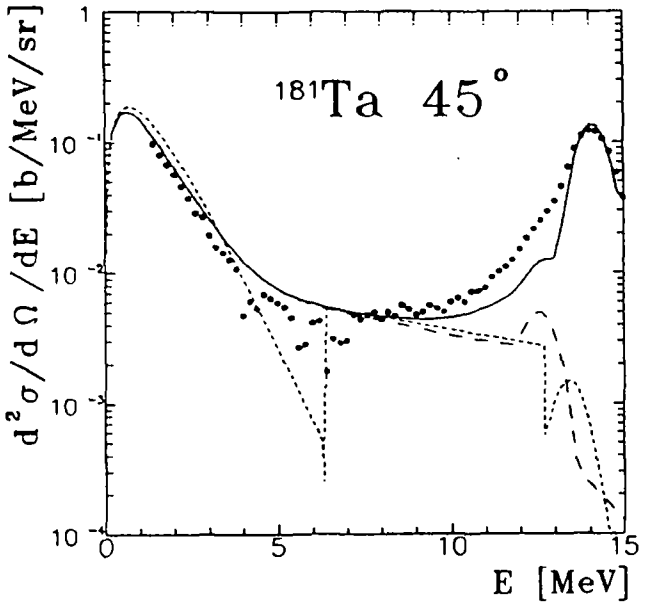

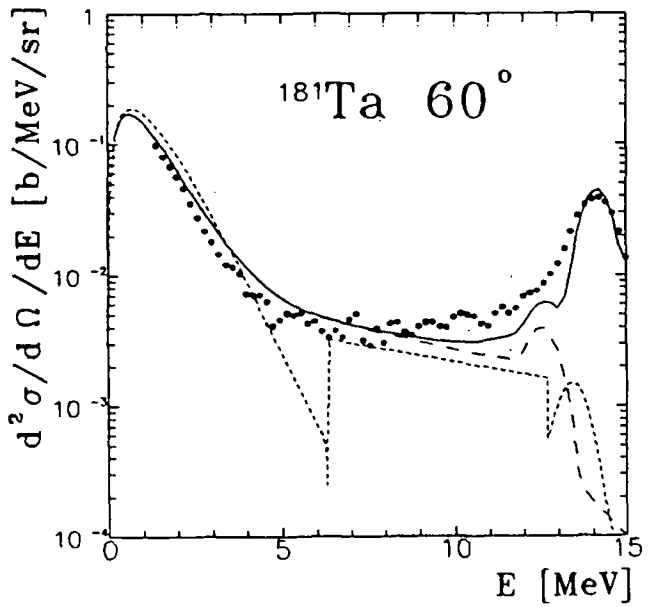

Fig. 5a)-i)

Double-differential neutron emission cross sections of tantalum at 14 MeV incidence energy.
Present experimental cross sections (•) are compared with ENDF/B-IV data (short-dashed line) and results of the EXIFON-calculation (long-dashed line). The solid line represents the sum of EXIFON results and the simulated elastic scattering peak.

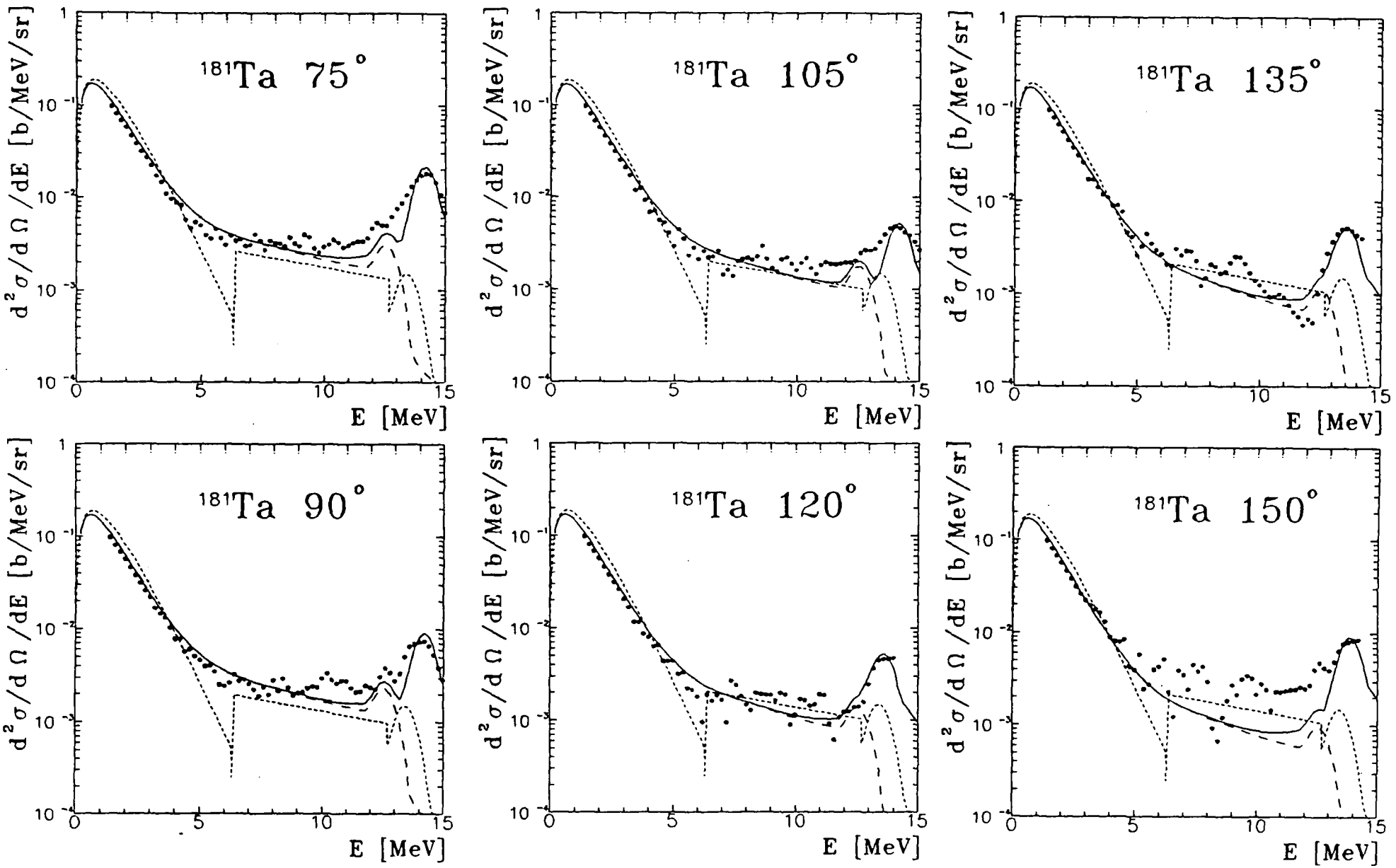
^{181}Ta 75°
^{181}Ta 105°
^{181}Ta 135°
^{181}Ta 90°
^{181}Ta 120°
^{181}Ta 150°
$d^2\sigma/d\Omega/dE$ [b/MeV/sr]
E [MeV]
1
10^{-1}
10^{-2}
10^{-3}
10^{-4}
0
5
10
15

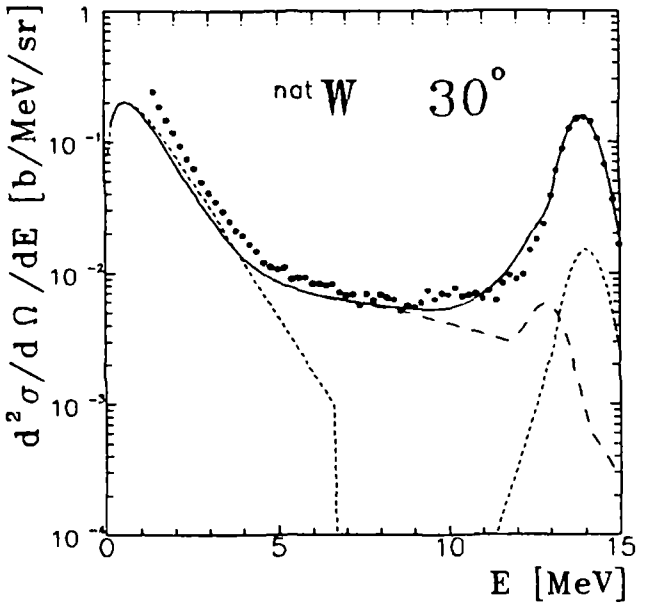

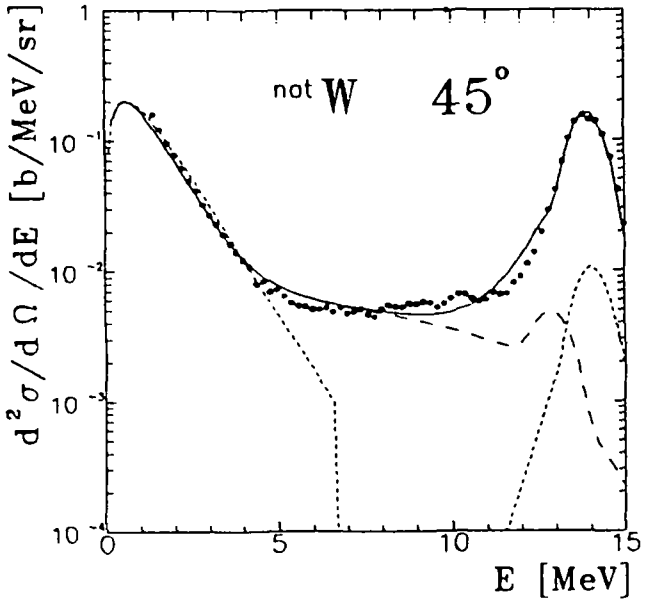

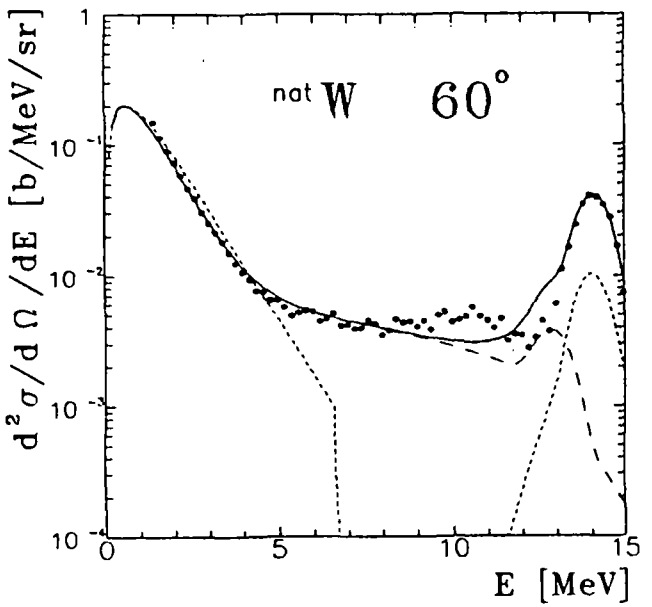

Fig. 6 a)-i)

Double-differential neutron emission cross sections of tungsten at 14 MeV incidence energy.
Present experimental cross sections (•) are compared with ENDF/B-IV data (short-dashed line) and results of the EXIFON-calculation (long-dashed line). The solid line represents the sum of EXIFON results and the simulated elastic scattering peak.

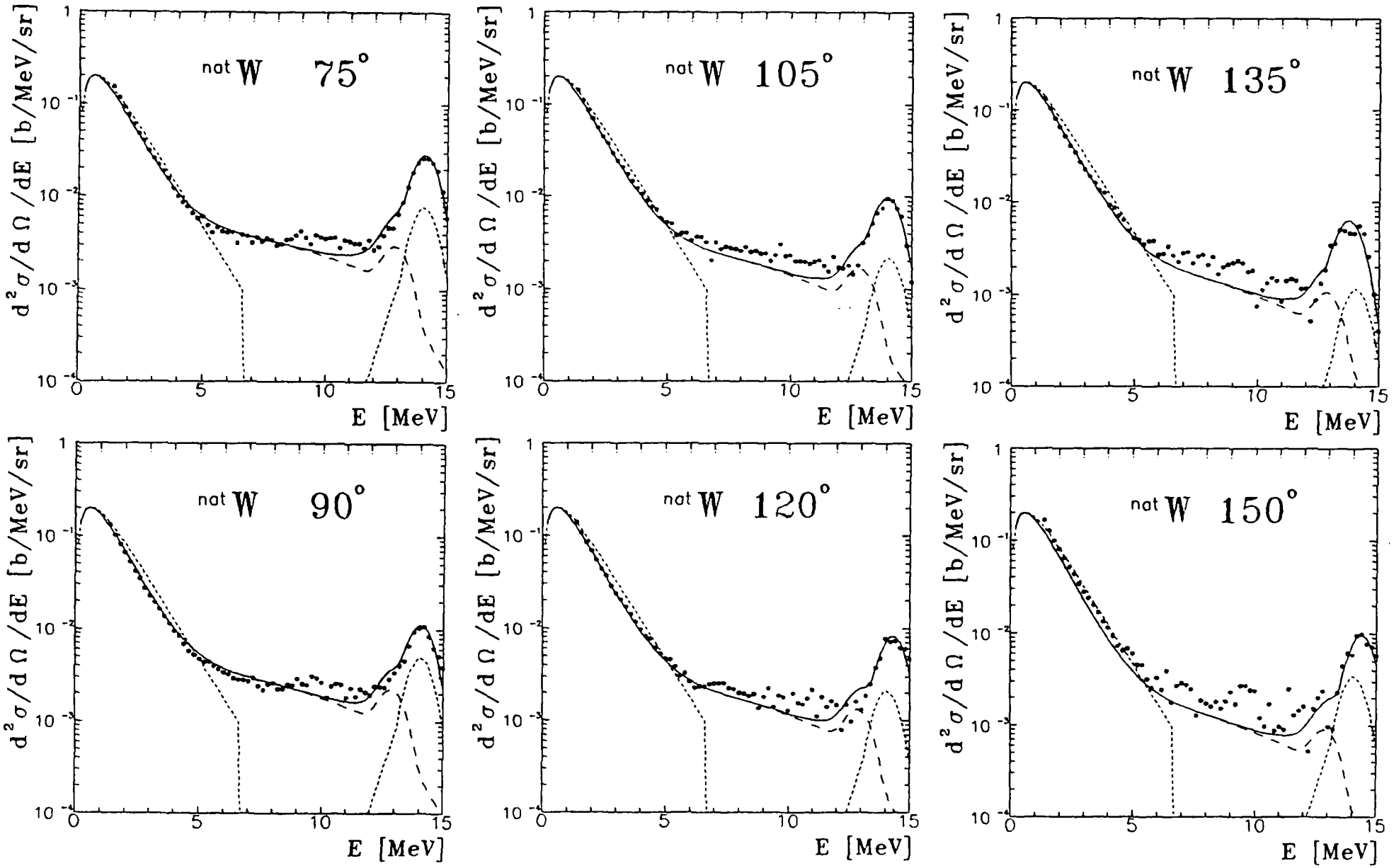
nat W 75°
nat W 105°
nat W 135°
nat W 90°
nat W 120°
nat W 150°
d²σ/dΩ/dE [b/MeV/sr]
E [MeV]
1
10⁻¹
10⁻²
10⁻³
10⁻⁴
0
5
10
15

References

/ 1/ World Request List for Nuclear Data, INDC(SEC)-095/URSF, IAEA, 1988.

/ 2/ K. Seidel and S. Unholzer; TUD-Informationen 05-09-82, TU Dresden, 1982.

/ 3/ T. Elfruth et al.; INDC(GDR)-044/GI, IAEA, Vienna, 1986.

/ 4/ R. Arlt et al.; ZfK-408(1979)154.

/ 5/ M. Adel-Fawzy et al.; ZfK-408(1979)150.

/ 6/ D. Hermsdorf; ZfK-315(1976)182.

/ 7/ M.B. Emmet; ORNL-4972(1975).

/ 8/ L.K. Penny, L.W. Owen; ORNL-TM-4007, ENDF/B-MAT 1196, 1972.

/ 9/ R.J. Howerton, et al.; LLL, ENDF/B-MAT 1285, 1974.

/10/ P. Rose and P. Young; LASL, ENDF/B-MAT 1128-1131, 1974.

/11/ A. Takahashi et al.; OKTAVIAN Report A-87-03, Osaka University (Japan), 1987.

/12/ A. Takahashi et al.; OKTAVIAN Report A-87-01, Osaka University (Japan), 1987.

/13/ A. Takahashi et al.; INDC(JPN)-118/L, IAEA,Vienna, 1989.

/14/ M. Baba et al.; Proc. 1987 Seminar on Nuclear Data, Tokai (Japan), JAERI-M-88-065(1988) p. 365.

/15/ H. Kalka et al.; Zeitschrift f. Physik A 335(1990)163.
H. Kalka et al.; Phys. Rev. C40(1989)1619.
H. Kalka; Proc. Int. School on Nucl. Physics, Kiev, 1990.

/16/ C. Kalbach, F.M.G. Mann; Phys. Rev. C23(1981)112.